

Hybrid stars : Spin polarised nuclear matter and density dependent quark masses

V.S. Uma Maheswari^{1,3}, J.N. De¹ and S.K. Samaddar²

¹ Variable Energy Cyclotron Centre,
1/AF, Bidhan Nagar, Calcutta - 700064, India

² Saha Institute of Nuclear Physics,
1/AF, Bidhan Nagar, Calcutta - 700064, India

³Institut für Theoretische Physik der Universität Tübingen,
Auf der Morgenstelle 14, D-72076 Tübingen, Germany

The possibility of formation of a droplet phase (DP) inside a star and its consequences on the structural properties of the star are investigated. For nuclear matter (NM), an equation of state (EOS) based on finite range, momentum and density dependent (FRMDD) interaction, and which predicts that neutron matter undergoes ferromagnetic transition at densities realisable inside the neutron star is employed. An EOS for quark matter (QM) with density dependent quark masses, the so-called effective mass model, is constructed by correctly treating the quark chemical potentials. A comparative study of hybrid star properties as obtained within the usual bag model and the effective mass model shows that both these models yield similar results. Then, the effect of spin polarisation on the formation of DP is investigated. Using the EOS based on FRMDD interaction alongwith the usual bag model, it is also found that a droplet phase consisting of strange quark matter and unpolarised nuclear matter sandwiched between a core of polarised nuclear matter and a crust containing unpolarised nuclear matter exists. Moreover, one could, in principle, explain the mass and surface magnetic field satisfactorily, and as well allow, due to the presence of a droplet phase, the direct URCA process to happen.

Keywords: Hybrid stars, Ferromagnetic phase in nuclear matter, Effective quark masses, Droplet phase

97.60.Jd; 21.65.+f

I. INTRODUCTION

Since the discovery of pulsars [1] and their identification [2] as rotating neutron stars during the late 1960's, much theoretical work have been done to study the structure of neutron stars. At the core of these objects, the density could be as high as five to ten times the nuclear matter density ($\rho_o \simeq 0.16 \text{ fm}^{-3}$) which falls down by several orders of magnitude in the crust region. The nature of matter at such high densities in the core is still an unresolved issue [3]. Over the two decades, many of the studies were addressed towards a resolution of this problem (see for e.g. [3,4]).

It has been conjectured in particular that there exists a phase transition between nuclear matter (NM) and quark matter (QM) at high densities [5-11]. Witten [12] has further speculated that the strange quark matter (SQM) consisting of u , d and s quarks may be the absolute ground state of hadronic matter. If this is true, then the possibility that pulsars are objects made up of purely SQM cannot be ruled out. Recently, from a semiempirical analysis of the mass-radius relationship Li *et al* [13] have suggested that Her X-1 pulsar maybe a strange quark star (see also [14]). On the basis of these hypotheses, several authors [3,5-11] have studied the properties of stars consisting of only SQM, *i.e.* strange quark stars (SQS) and neutron stars having quark cores with nucleon envelopes, *viz.* hybrid stars (HS). In general, the transition between the nuclear and quark matter is considered to occur at a unique pressure determined by Gibbs criteria, (we consider the transition to be first order). Inside the star, the pressure decreases smoothly outwards. The mixed phase has constant pressure independent of the volume fraction of the phases and therefore, the mixed phase collapses to a single point on the density profile of the star. Consequently, the mixed phase cannot exist in the hybrid star. Glendenning [15] has recently proposed that for systems with more than one conserved charge, the QM and NM could coexist for a finite range of pressures. A well-defined mixed phase may therefore be present [15-17] over a finite region within the star (hereafter referred to as the droplet phase).

Occurrence of a droplet phase (DP) have quite important observational consequences. In particular, the values of β -equilibrated proton fraction x_p in DP can be large enough to allow direct URCA process to happen, and hence, is of significance to the cooling process of neutron stars. However, whether or not such a DP is energetically favourable

depends largely upon the nature of dense matter. As yet, the exact nature of dense nuclear matter is not known, and several possibilities are equally probable. Very recently, we had shown [18], using a well-defined, finite range, momentum and density dependent interaction, that pure neutron matter undergoes a ferromagnetic phase transition at density $\rho \sim 4\rho_0$. Using such an equation of state, we then made a detailed study of structural properties of neutron and hybrid stars, and showed that one could, in principle, explain both the surface magnetic field and the standard structural properties. An interesting result is that β -equilibrated proton fraction x_p decreases sharply once the star matter becomes spin polarised (see Fig. 5 of Ref. [18]). One then naturally wonders, what is the effect of such phase transitions on the occurrence and properties of DP? In particular, whether or not ferromagnetic domains, *i.e.* droplets of spin polarised matter, exist inside a star. And, what is the role of spin polarisation in the determination of x_p , and thereby, on the possibility of direct URCA process. In view of these, we mainly investigate the following. Firstly, whether the proposed equation of state, based on an interaction with firm basis in the well known properties of nuclear matter and finite nuclei, which predicts a ferromagnetic phase transition permits a droplet phase. Secondly, if such a phase is allowed, what are the effects of spin polarisation on the star structure? Finally, can one consistently describe the standard structural properties and surface magnetic field, as well as find the finite probability for the direct URCA process to happen?

Now, in addition to the properties of dense nuclear matter, the nature of the quark matter equation of state can also affect the possibility of formation of a droplet phase. The theoretical framework that has been used in general to study HS and SQS is the MIT bag model [19]. In this model, the non-perturbative aspects of quark-quark interaction, *i.e.* the confinement property is invoked through a bag parameter. An alternate way of implementing confinement has also been explored [20–22], which is hereafter referred to as effective mass model of confinement. In this approach, the quark masses are assumed to be density dependent. In the limit of high densities, their values tend towards the current quark masses; in the limit of zero density, the quark masses become infinite. Attempts have been made [23,24] to study the properties of SQS in this approach. In Ref. [23], it was noted that the properties of SQM obtained using the density dependent quark masses are quite different from those obtained using the MIT bag model. This was subsequently contested in Ref. [24], where it was found that both the approaches yield similar results. An intriguing aspect in the latter study is that the pressure does not vanish at the density where the energy per baryon has a minimum. This contradicts the very definition of the ground state of a system. As shown in the following section, both these studies have incorrectly determined the quark chemical potentials. Due to the explicit density dependence of quark masses, there is an extra term, the so-called rearrangement energy, in the definition of chemical potential. Taking this term into account, it is shown that the energy minimum and zero pressure occur at the same density point. Further, we make a comparative study of properties of hybrid stars as obtained using the effective mass model and bag model of quark confinement.

It may also be said here that in addition to the bulk properties of the equations of state, the finite size effects [16,25] such as Coulomb, surface and curvature contributions can affect the possible formation of the droplet phase inside a star. However, it is known that surface tension of QM is poorly determined [16], and is also found to be dependent upon the shape of the confining potential [26]. Moreover, the internal structure of the droplet phase is generally determined by the competition between the Coulomb and surface energies, and can adopt shapes like rods, plates and spheres [16]. Here, since we are mainly concerned with the effect of spin polarisation in the formation of the droplet phase, the finite size effects are presently not considered.

II. THEORETICAL FRAMEWORK FOR QUARK MATTER EOS

In the following, we briefly outline the procedure to obtain the quark equation of state in the effective mass approximation.

A. The effective mass approximation

The two important properties of QCD, namely the asymptotic freedom and the confinement, are adequately represented by considering that quarks are bound by a local Dirac-scalar potential, $S(\vec{r}) \sim c_l |\vec{r}|^l$ [27,28]. Presence of a strong Dirac-scalar component is found to be consistent with the concept of chiral symmetry [29]. In terms of $S(\vec{r})$, one can then define the quark effective mass as $m_q(\vec{r}) = m_q^0 + c_l |\vec{r}|^l$ [28,30]. Its average value in the bulk matter limit is taken to be of the form,

$$m_q = \langle m_q(\vec{r}) \rangle \equiv m_q^0 + C\rho_b^{-n} \quad ; \quad n = l/3 > 0, \quad (1)$$

where m_q^0 is the current quark mass, ρ_b is the baryon number density and C and n are parameters to be determined by requiring that strange quark matter is stable or unstable against the normal nuclear matter. In this effective mass model, quark-quark interactions are assumed to be included through the density dependence of the quark masses. Further, Eq. (1) implies that in the asymptotically free regime, *i.e.* at high densities, $m_q \rightarrow m_q^0$, the current quark mass. In the limit $\rho_b \rightarrow 0$, $m_q \rightarrow \infty$; this gives rise to absolute confinement.

B. Rearrangement energy and Hugenholtz-Van Hove theorem

Consider a system of one kind of quarks with an effective mass m_q defined in Eq. (1). Then, the total quark number N_q and the energy E_q of the given system are determined using the expressions:

$$\begin{aligned} N_q &= \sum_k n(k), \\ E_q &= \sum_k n(k) \sqrt{k^2 + m_q^2}, \end{aligned} \quad (2)$$

where k is the momentum and m_q is in units of $\hbar c$, with $\hbar = c = 1$. The occupation probability function $n(k)$, at a given temperature T is

$$n(k) = \left[1 + \exp\left(\frac{\epsilon_k - \mu_q}{T}\right) \right]^{-1}, \quad (3)$$

where μ_q is the quark chemical potential. The single particle energies ϵ_k are determined using the standard definition, $\epsilon_k = \partial E_q / \partial n(k)$. In the limit of zero temperature, one gets,

$$\begin{aligned} \epsilon_k &= \sqrt{k^2 + m_q^2} + \frac{g}{4\pi^2} \frac{\partial m_q}{\partial \rho_q} [m_q k_F \sqrt{k_F^2 + m_q^2} - \\ & m_q^3 \ln\left(\frac{k_F + \sqrt{k_F^2 + m_q^2}}{m_q}\right)], \\ &\equiv \sqrt{k^2 + m_q^2} + U(\rho_q), \end{aligned} \quad (4)$$

where $\rho_q (= 3\rho_b)$ is the quark number density and the spin-colour degeneracy factor $g = 6$. The term $U(\rho_q)$ in Eq. (4) arises solely due to the density dependence of quark mass. In the context of nuclear physics, such a term is normally referred to as the rearrangement energy [31,32]. Because of this term, the single particle levels depend explicitly upon the value of the Fermi momentum k_F . In the limit $T \rightarrow 0$, one can obtain from Eq. (4) the chemical potential μ_q , equivalently the Fermi energy ϵ_F to be

$$\epsilon_F \equiv \mu_q |_{T=0} = \sqrt{k_F^2 + m_q^2} + U(\rho_q). \quad (5)$$

Similarly, the quark number density $\rho_q = N_q/V$ and the energy density $\epsilon_q = E_q/V$ are determined using Eq. (2) as

$$\begin{aligned} \rho_q &= \frac{g k_F^3}{6\pi^2}, \\ \epsilon_q &= \frac{g}{16\pi^2} [(2k_F^3 + m_q^2 k_F) \sqrt{k_F^2 + m_q^2} - \\ & m_q^4 \ln\left(\frac{k_F + \sqrt{k_F^2 + m_q^2}}{m_q}\right)], \end{aligned} \quad (6)$$

where V is the total volume of the system. In the limit $C \rightarrow 0$, $U(\rho_q) \rightarrow 0$, and one arrives at the usual Fermi gas model expressions for μ_q and ϵ_q . Starting with the standard definition (2) for energy, one thus arrives at a new feature in the expression for μ_q in the effective mass approximation as compared to the bag model.

We now demonstrate that Eqs. (5) and (6) are consistent with the well-known Hugenholtz-Van Hove (HVH) theorem [33] arrived at in the context of interacting Fermi systems. The HVH theorem in general deals with the

single particle properties of an interacting Fermi gas at $T = 0$. For a system of one kind of particles, the theorem states that

$$\mu_q = \epsilon_F = \left(\frac{\partial E_q}{\partial N_q} \right)_V. \quad (7)$$

It is straightforward to see that $(\partial E_q / \partial N_q)_V = E_q / N_q + \rho_q [\partial (E_q / N_q) / \partial \rho_q]_V$. Then at equilibrium, *i.e.* at the density corresponding to zero pressure one has as a special case, $\mu_q = E_q / N_q$. Thus, it relates the quark chemical potential at equilibrium to the average energy per particle.

Using Eqs. (6) and (7), we then obtain,

$$\begin{aligned} \mu_q &= \left(\frac{\partial E_q}{\partial N_q} \right)_V, \\ &= \frac{\partial \epsilon_q}{\partial \rho_q}, \\ &= \sqrt{k_F^2 + m_q^2} + U(\rho_q), \end{aligned} \quad (8)$$

which is same as in Eq. (5) demonstrating the consistency with the HVH theorem. The results are equally true for multicomponent quark systems also. We do this exercise in order to emphasize that earlier studies [23,24] do not include such a rearrangement term in their definitions of μ_q .

C. The equation of state

Here, we construct, within the effective mass approximation, the equation of state of β -equilibrated, electrically neutral quark matter.

The total kinetic energy density of a system of non-interacting, relativistic quarks of flavour τ and effective mass m_τ is given as,

$$\epsilon_\tau = \frac{3}{8\pi^2} \frac{(m_\tau c^2)^4}{(\hbar c)^3} \left[x_\tau \sqrt{1 + x_\tau^2} (1 + 2x_\tau^2) - \ln(x_\tau + \sqrt{1 + x_\tau^2}) \right], \quad (9)$$

where $x_\tau = p_F^\tau / (m_\tau c)$, p_F^τ is the Fermi momentum and is related to the quark number density ρ_τ of a given flavour as $p_F^\tau = \hbar(\pi^2 \rho_\tau)^{1/3}$. The densities pertaining to the three flavours can be expressed in terms of the total quark number density ρ_q and the asymmetry parameters δ_{ud} and δ_{us} as:

$$\begin{aligned} \rho_u &= (\rho_q/3) [1 - \delta_{ud} - \delta_{us}] \equiv (\rho_q/3) f_u, \\ \rho_d &= (\rho_q/3) [1 + 2\delta_{ud} - \delta_{us}] \equiv (\rho_q/3) f_d, \\ \rho_s &= (\rho_q/3) [1 - \delta_{ud} + 2\delta_{us}] \equiv (\rho_q/3) f_s, \end{aligned} \quad (10)$$

where $\delta_{ud} = (\rho_d - \rho_u) / \rho_q$, $\delta_{us} = (\rho_s - \rho_u) / \rho_q$ and $\rho_q = \rho_u + \rho_d + \rho_s = 3\rho_b$. Similarly, the energy density ϵ_L pertaining to a system of relativistic non-interacting electron gas is obtained as

$$\epsilon_L = \frac{1}{8\pi^2} \frac{(m_e c^2)^4}{(\hbar c)^3} \left[x_e \sqrt{1 + x_e^2} (1 + 2x_e^2) - \ln(x_e + \sqrt{1 + x_e^2}) \right], \quad (11)$$

where $x_e = p_{F,e} / (m_e c)$, $m_e = 0.511$ MeV, and $p_{F,e}$ is the electron Fermi momentum related to the density ρ_e as $p_{F,e} = \hbar(3\pi^2 \rho_e)^{1/3}$.

The equilibrium composition of the quark matter is then determined subject to the β -equilibrium conditions,

$$\mu_d - \mu_u = \mu_e \quad \text{and} \quad \mu_d = \mu_s, \quad (12)$$

and the charge neutrality condition,

$$\rho_e = \frac{1}{3} (2\rho_u - \rho_d - \rho_s). \quad (13)$$

Using Eq. (10) one obtains, $\rho_e = -(\rho_q/3) (\delta_{ud} + \delta_{us})$. Similarly, one can express the chemical potentials μ_u , μ_d and μ_s in terms of the three quantities ρ_q , δ_{ud} and δ_{us} as follows:

$$\begin{aligned}\mu_u &= \left(\frac{\partial \epsilon_q}{\partial \rho_u} \right)_{\rho_d, \rho_s} = \frac{\partial \epsilon_q}{\partial \rho_q} - \frac{1 + \delta_{ud}}{\rho_q} \frac{\partial \epsilon_q}{\partial \delta_{ud}} - \frac{1 + \delta_{us}}{\rho_q} \frac{\partial \epsilon_q}{\partial \delta_{us}}, \\ \mu_d &= \left(\frac{\partial \epsilon_q}{\partial \rho_d} \right)_{\rho_u, \rho_s} = \frac{\partial \epsilon_q}{\partial \rho_q} + \frac{1 - \delta_{ud}}{\rho_q} \frac{\partial \epsilon_q}{\partial \delta_{ud}} - \frac{\delta_{us}}{\rho_q} \frac{\partial \epsilon_q}{\partial \delta_{us}}, \\ \mu_s &= \left(\frac{\partial \epsilon_q}{\partial \rho_s} \right)_{\rho_u, \rho_d} = \frac{\partial \epsilon_q}{\partial \rho_q} - \frac{\delta_{ud}}{\rho_q} \frac{\partial \epsilon_q}{\partial \delta_{ud}} + \frac{1 - \delta_{us}}{\rho_q} \frac{\partial \epsilon_q}{\partial \delta_{us}},\end{aligned}\quad (14)$$

where $\epsilon_q = \sum_{\tau} \epsilon_{\tau}$ is the total quark energy density ; $\tau = u, d, s$. The various energy derivatives occurring in Eq. (14) are given by

$$\begin{aligned}\left(\frac{\partial \epsilon_q}{\partial \rho_q} \right)_{\delta_{ud}, \delta_{us}} &= \mu_q = \frac{1}{3} \sum_{\tau} \lambda_{\tau} f_{\tau} + \sum_{\tau} U_{\tau}, \\ \left(\frac{\partial \epsilon_q}{\partial \delta_{ud}} \right)_{\rho_q, \delta_{us}} &= \frac{\rho_q}{3} \sum_{\tau} \lambda_{\tau} \left(\frac{\partial f_{\tau}}{\partial \delta_{ud}} \right)_{\delta_{us}}, \\ \left(\frac{\partial \epsilon_q}{\partial \delta_{us}} \right)_{\rho_q, \delta_{ud}} &= \frac{\rho_q}{3} \sum_{\tau} \lambda_{\tau} \left(\frac{\partial f_{\tau}}{\partial \delta_{us}} \right)_{\delta_{ud}},\end{aligned}\quad (15)$$

where $f_{\tau} = \rho_{\tau}/\rho_b$,

$$U_{\tau} = \frac{3}{2\pi^2} \left(\frac{m_{\tau} c}{\hbar} \right)^3 \frac{\partial m_{\tau}}{\partial \rho_q} \left[x_{\tau} \sqrt{1 + x_{\tau}^2} - \ln(x_{\tau} + \sqrt{1 + x_{\tau}^2}) \right], \quad (16)$$

and $\lambda_{\tau} = m_{\tau} c^2 \sqrt{1 + x_{\tau}^2}$ is the chemical potential of the quarks with density independent masses which is also the usual bag model result. The chemical potentials corresponding to each flavour (14) can also be expressed as follows:

$$\mu_{\tau} = \lambda_{\tau} + \sum_{\tau'} U_{\tau'}. \quad (17)$$

Then using Eq. (14), the β -equilibrium conditions (12) can be expressed in terms of the asymmetry parameters as

$$\begin{aligned}\frac{\partial \epsilon_q}{\partial \delta_{ud}} - \frac{\partial \epsilon_q}{\partial \delta_{us}} &= 0, \\ \frac{2}{\rho_q} \frac{\partial \epsilon_q}{\partial \delta_{ud}} + \frac{1}{\rho_q} \frac{\partial \epsilon_q}{\partial \delta_{us}} &= \mu_e,\end{aligned}\quad (18)$$

where $\mu_e = \sqrt{p_{F,e}^2 c^2 + m_e^2 c^4}$. From Eq. (17), the same can be reexpressed as

$$\lambda_d - \lambda_s = 0 \quad \text{and} \quad \lambda_d - \lambda_u = \mu_e. \quad (19)$$

Thus, for a given baryon density $\rho_b = \rho_q/3$, the three quantities ρ_e , δ_{ud} and δ_{us} are fixed by the Eqs. (13) and (18). The total energy density of quark matter ϵ_{QM} and the pressure P_{QM} for a given ρ_b are then given as

$$\begin{aligned}\epsilon_{\text{QM}} &= \sum_{\tau} \epsilon_{\tau}(\rho_q, \delta_{ud}, \delta_{us}) + \epsilon_L(\rho_q, \delta_{ud}, \delta_{us}), \\ P_{\text{QM}} &= \rho_q \frac{\partial \epsilon_{\text{QM}}}{\partial \rho_q} - \epsilon_{\text{QM}}.\end{aligned}\quad (20)$$

Eq. (20) defines the equation of state of charge neutral, β -equilibrated quark matter.

In order to make a comparative study, we also consider the bag model picture. The quark matter equation of state within the bag model can be determined from Eq. (20) itself by setting $C = 0$, and adding a bag energy density B to the total energy density ϵ_{QM} . One then gets,

$$\begin{aligned}\epsilon_{\text{bag}} &= \epsilon_{\text{QM}}[C = 0] + B, \\ P_{\text{bag}} &= \rho_q \frac{\partial \epsilon_{\text{bag}}}{\partial \rho_q} - \epsilon_{\text{bag}}.\end{aligned}\quad (21)$$

Before, we discuss the results obtained within these two models, we give below the equations of state considered for nuclear matter.

III. NUCLEAR MATTER EQUATION OF STATE

A. A simple parametrisation

For the comparative study of properties of hybrid stars within the bag and effective mass models, we choose a simple parametrisation of nuclear matter EOS as given in Ref. [16]. The total energy density ϵ_n for a system of neutrons and protons is taken to be of the form,

$$\epsilon_n = \rho_b [M_n + E_{\text{comp}} + E_{\text{sym}}], \quad (22)$$

where M_n is the nucleon mass. The compressional energy is given by $E_{\text{comp}} = (K_o/18)(\rho_b/\rho_o - 1)^2$ and the symmetry energy is $E_{\text{sym}} = S_o (\rho_b/\rho_o) (1 - 2x_p)^2$, where x_p is the proton fraction. Values for the nuclear matter incompressibility K_o , symmetry energy coefficient S_o and the normal nuclear matter density ρ_o are taken to be 250 MeV, 30 MeV and 0.16 fm^{-3} respectively [16].

The optimum value of x_p for a given ρ_b is determined by the β - equilibrium condition and the charge neutrality condition:

$$\mu_n = \mu_p + \mu_e \quad \text{and} \quad \rho_e = x_p \rho_b, \quad (23)$$

where μ_n and μ_p are the neutron and proton chemical potentials respectively. The total energy density ϵ_{NM} and pressure P_{NM} corresponding to nuclear matter for a given baryon density ρ_b is then given as,

$$\begin{aligned} \epsilon_{\text{NM}} &= \epsilon_n(\rho_b, x_p) + \epsilon_L(\rho_b, x_p), \\ P_{\text{NM}} &= \rho_b \frac{\partial \epsilon_{\text{NM}}}{\partial \rho_b} - \epsilon_{\text{NM}}. \end{aligned} \quad (24)$$

The above equation defines the equation of state of the β - equilibrated, charge neutral nuclear matter.

B. Based on a realistic interaction with explicit spin degrees of freedom

The phenomenological momentum and density dependent finite range interaction employed here to obtain the equation of state is a modified version of Seyler-Blanchard interaction [32]. To treat spin-polarised isospin asymmetric nuclear matter, the interaction has been generalised to include explicitly the spin-isospin dependent channel. The interaction between two nucleons with separation r and relative momentum p is given by,

$$v_{\text{eff}}(r, p, \rho) = -C_{\tau s} \left[1 - \frac{p^2}{b^2} - d^2(\rho_1(r_1) + \rho_2(r_2))^\gamma \right] \frac{e^{-r/a}}{r/a}, \quad (25)$$

where a is the range and b defines the strength of the repulsion in the momentum dependence of the interaction. The parameters d and γ are measures of the strength of the density dependence, and ρ_1 and ρ_2 are the densities at the sites of the two interacting nucleons. The subscripts τ and s in the strength parameter $C_{\tau s}$ refer to the likeness l and the unlikeness u in the isotopic spin and spin of the two nucleons respectively; for example, C_{ll} refers to interactions between two neutrons or protons with parallel spins, C_{lu} refers to that between neutrons or protons with opposite spin *etc.* The energy per nucleon E/A and the pressure P in the mean-field approximation can then be worked out [32] as

$$E/A = \frac{1}{\rho} \sum_{\tau s} \rho_{\tau s} \left[T \frac{J_{3/2}(\eta_{\tau s})}{J_{1/2}(\eta_{\tau s})} (1 - m_{\tau s}^* V_{\tau s}^1) + \frac{1}{2} V_{\tau s}^0 \right], \quad (26)$$

$$P = \sum_{\tau s} \rho_{\tau s} \left[\frac{2}{3} T \frac{J_{3/2}(\eta_{\tau s})}{J_{1/2}(\eta_{\tau s})} + V_{\tau s}^0 + \frac{1}{2} b^2 (1 - d^2(2\rho)^\gamma) V_{\tau s}^1 + V_{\tau s}^2 \right]. \quad (27)$$

Here, $J_k(\eta)$ are the Fermi integrals, $V_{\tau s}^0$ and $V_{\tau s}^2$ are the single-particle and the rearrangement potentials, $V_{\tau s}^1$ is the coefficient of the quadratic momentum dependent term in the potential and defines the effective mass $m_{\tau s}^*$, T the temperature, and η is the fugacity given by $\eta_{\tau s} = (\mu_{\tau s} - V_{\tau s}^0 - V_{\tau s}^2)/T$. For the unpolarised nuclear matter (UNM),

the expressions for $V_{\tau s}^0$ etc are given in ref. [32]. It is straightforward to extend these to the case of polarised nuclear matter (PNM) and are given in detail in Ref. [18].

One usually defines the neutron and proton spin excess parameters (spin asymmetry) as

$$\begin{aligned}\alpha_n &= (\rho_{n\uparrow} - \rho_{n\downarrow})/\rho, \\ \alpha_p &= (\rho_{p\uparrow} - \rho_{p\downarrow})/\rho,\end{aligned}\tag{28}$$

where

$$\rho = \rho_n + \rho_p = (\rho_{n\uparrow} + \rho_{n\downarrow}) + (\rho_{p\uparrow} + \rho_{p\downarrow}),\tag{29}$$

is the number density. We then define the proton fraction as $x = \rho_p/\rho$. It is related to the isospin asymmetry parameter X as,

$$X = (1 - 2x) = (\rho_n - \rho_p)/\rho.\tag{30}$$

We also define the spin excess parameter as $Y = \alpha_n + \alpha_p$ and the spin-isospin excess parameter as $Z = \alpha_n - \alpha_p$. One can then express the energy per nucleon E/A of the NM at zero temperature as

$$E/A = E_V + E_X X^2 + E_Y Y^2 + E_Z Z^2,\tag{31}$$

where terms higher than those quadratic in X , Y and Z are neglected. Here E_V is the volume energy of the symmetric nuclear matter, taken as -16.1 MeV and E_X is the usual symmetry (isospin) energy, taken to be 33.4 MeV. The quantities E_Y and E_Z are the spin and the spin-isospin symmetry energies of the NM respectively. We take [34,35,18] $E_X = 33.4$ MeV, $E_Y = 15$ MeV and $E_Z = 36.5$ MeV. Values of these coefficients are uncertain to an extent.

The generalised hydrodynamical model of Uberall [36], which gives $(E_Z/E_X)^{1/2} \simeq 1.1$ fixes E_Z for a given value of E_X . The value of E_Y is relatively more uncertain, and it was found in our earlier study [18] on neutron stars that standard neutron star properties are best explained with $E_Y = 15$ MeV and hence we use here the same set of parameters. The values of the parameters $C_{\tau s}$, a , b , d and γ are then determined by reproducing E_V , E_X , E_Y , E_Z , the saturation density of normal nuclear matter ($\rho_0 = 0.1533 \text{ fm}^{-3}$), the surface energy coefficient ($a_S = 18.0$ MeV), the energy dependence of the real part of the nucleon-nucleus optical potential and the breathing-mode energies [37]. The parameters of the interaction so determined are listed below:

$$\begin{aligned}C_{ll} &= -305.2 \text{ MeV} & a &= 0.625 \text{ fm} \\ C_{lu} &= 902.2 \text{ MeV} & b &= 927.5 \text{ MeV}/c \\ C_{ul} &= 979.4 \text{ MeV} & d &= 0.879 \text{ fm}^{3n/2} \\ C_{uu} &= 776.2 \text{ MeV} & \gamma &= 1/6.\end{aligned}$$

With the above value of the parameter γ , the incompressibility of symmetric nuclear matter is $K = 240$ MeV.

It may be said here that the above interaction reproduces quite well the ground state binding energies, root mean square charge radii, charge distributions and giant monopole resonance energies for a host of even-even nuclei ranging from ^{16}O to very heavy systems. We have also seen that for symmetric nuclear matter, our results agree extremely well with those calculated in a variational approach by Friedmann and Pandharipande(FP) [38] with $v_{14} + TNI$ interaction in the density range $\frac{1}{2}\rho_0 \leq \rho \leq 2\rho_0$. But, for unpolarised pure neutron matter, the energies calculated [18] with our interaction are somewhat higher compared to the FP energies, particularly at higher densities. However, our results [18] are very similar to those obtained from the recent sophisticated calculation of Wiringa et al [39] with UV14+UVII interaction, and hence the present interaction can be extrapolated with some confidence to neutron matter at high densities. Then, using this interaction it was found [18] that neutron matter undergoes a ferromagnetic transition at a density $\rho \sim 4\rho_0$. Before, we investigate the effect of such a ferromagnetic transition on neutron star properties, certain general aspects of SQM as obtained within the effective mass model of confinement is discussed below.

IV. FLAVOUR SYMMETRIC STRANGE QUARK MATTER

Having clearly specified, in the above two sections, the various equations of state considered for quark matter and nuclear matter, we are now in a position to make a detailed study of hybrid stars. To do so, firstly, we would like to demonstrate the consistency of our present QM calculation done within the effective mass model, and as well make a preliminary study of the general aspects of the strange quark matter equation of state given by Eq. (20). For this

purpose, we take the current quark masses of u , d and s to be zero. As the parameters n and C (defined in Eq. (1)) by the density dependence of the quark masses) are flavour independent, the quark masses are the same and hence, the matter is flavour symmetric, *i.e.* $f_u = f_d = f_s = 1$.

The mass parameters n and C are chosen so that at the density where pressure $P = 0$, $(M/A)_{P=0} < 930$ MeV. Here M/A is the total mass per baryon of the flavour symmetric SQM. In Table 1, the values of $(M/A)_{P=0}$ so-obtained are shown for several values of n and C . The main result of this preliminary investigation is shown in Fig. 1, where we have plotted M/A and P as a function of the baryon density ρ_b . Values of n and C are taken to be $2/3$ and 85 MeV fm^{-2} . As expected, the minimum of M/A and $P = 0$ occurs at the same density point for all values of n and C considered here. It may be noted that in the study in Ref. [24], the above mentioned density points did not coincide; this could be due to the noninclusion of the rearrangement term in the single particle energy. The role of this rearrangement energy in quark chemical potential is illustrated in Fig. 2, where the ratio μ_d/λ_d is displayed as a function of baryon density ρ_b . The chemical potentials λ_d and μ_d are as defined in Eq. (17). The deviation from unity in the case of the effective mass model is due to the rearrangement term. The effect of this term is dominant in the low density regime. As the density ρ_b increases, $\mu_d/\lambda_d \rightarrow 1$, the bag model result; this is due to the fact that as $\rho_b \rightarrow \infty$, $m_\tau \rightarrow m_\tau^0$, and hence the rearrangement term $U_\tau \rightarrow 0$ as can be seen from Eq. (16). Similar curves for other flavours are not shown as $\mu_s/\lambda_s = \mu_d/\lambda_d = \mu_u/\lambda_u$.

We have also studied the dependence of the properties of strange quark star on the mass parameters n and C . The total mass and the radius of the star are obtained by solving the general relativistic Tolman-Oppenheimer-Volkoff (TOV) equation [4],

$$\frac{dP(r)}{dr} = -\frac{G}{c^4} \frac{[\epsilon(r) + P(r)] [m(r)c^2 + 4\pi r^3 P(r)]}{r^2 \left[1 - \frac{2Gm(r)}{rc^2}\right]}, \quad (32)$$

where,

$$m(r)c^2 = \int_0^r \epsilon(r') d^3 r'. \quad (33)$$

The quantities $\epsilon(r)$ and $P(r)$ are the energy density and pressure at a radial distance r from the centre of the star, and are given by the equation of state (20). The mass of the star contained within a distance r is given by $m(r)$. The size of the star is determined by the boundary condition $P(R) = 0$ and the total mass M of the star integrated upto the surface R is given by $M = m(R)$. The single integration constant needed to solve the TOV equation is P_c , the pressure at the center of the star calculated at a given central density ρ_c . The values of the total mass M_{\max} and the radius R of the star corresponding to the maximum mass configuration are given in Table 1. The central density ρ_c in units of ρ_o is also given. In order to understand the behaviour of the various structural properties of SQS with respect to the change in the mass parameters n and C , we have calculated the incompressibility $K_q = (dP/d\rho_q)$ of the star matter, which is displayed in Fig. 3 as a function of ρ_b for three sets of (n, C) . It is found that with increase in n (keeping C fixed), the EOS becomes stiffer. With n fixed, if C is increased, the EOS becomes effectively a little stiffer (averaged over the density of the star) though at low densities, it is somewhat softer. From Table 1, we note that as the EOS becomes stiffer, $(M/A)_{P=0}$ and ρ_c increases whereas R and M_{\max} decreases. These results corroborate the findings by Haensel et al [10] in the bag model. We expect these features to be valid even when the β -equilibrium conditions are considered, since it is in general found [10] that β -equilibrated SQM is nearly flavour symmetric and the electron density is negligibly small.

Finally, taking into account both β -equilibrium and charge neutrality conditions given by equations (12) and (13) respectively, we determined the mass-radius relationship of the strange quark star by solving the TOV equation in both the models described by Eqs. (20) and (21). Results so obtained are displayed in Fig. 4 and it can be seen that results obtained within the two models of quark confinement are quite similar. It may be stressed here that the values of M_{\max} and R are dependent on the model parameters. It is found that with suitable choice of the parameters, it is possible to obtain the maximum mass and the radius of the star well within the acceptable limits. For the sake of comparison, we have shown the results obtained for a neutron star in the same figure. The structure of the neutron star is determined using a composite EOS, *i.e.* Feymann-Metropolis-Teller [40], Baym-Pethick-Sutherland [41], Baym-Bethe-Pethick [42] and that given by Eqs. (26-27) with progressively increasing densities. It is already known from previous studies [10] that curvature of the $M - R$ curves in the low mass region as obtained from the bag model for SQS is opposite to that of the neutron star. This difference is also borne out in the present calculation using effective quark masses. Thus, our present calculation of quark matter EOS within effective mass model is consistent with the general findings in literature.

V. HYBRID STARS : A COMPARATIVE STUDY OF TWO MODELS OF QUARK CONFINEMENT

Strange quark matter may not be the absolute ground state of hadronic matter. If this is so, then it is possible that neutron stars are not made up of only quark matter, but have a quark core enveloped by nuclear matter, usually referred to as hybrid stars. Since the quark-hadron transition is normally taken to be of first order, there exists a mixed phase consisting of droplets of quark matter and of nuclear matter in thermodynamic equilibrium. As this occurs at a unique pressure, such a phase cannot exist inside the hybrid star. Taking into account the recent viewpoint of Glendenning [15] as already mentioned in the introduction, the existence of this droplet phase inside the hybrid star cannot however be ruled out. In this section, we investigate the structure of this droplet phase and its observable consequences on the structural properties of the neutron star using the two models of quark confinement, *viz* bag and effective mass models. We thereby perform calculations similar to the earlier studies [24,23], but with the correct treatment of quark chemical potentials. Moreover, we make use of the simple parametrisation of nuclear matter EOS given by Eq. (24) in order to be able to directly compare our results to those obtained in earlier studies [16,23].

A. Equation of state for droplet phase

We consider the droplet phase to be present in a uniform background [16] of electron gas. The system as a whole is charge neutral, and each phase of matter is subjected to appropriate β -equilibrium conditions.

For the nuclear matter phase, we consider the EOS as given by Eq. (24). The appropriate β -equilibrium condition is $\mu_n = \mu_p + \mu_e$. The total charge density ρ_z^N pertaining to the NM phase is given by $\rho_z^N = \rho_p - \rho_e = x_p \rho_b^N - \rho_e$, where ρ_p is the proton density and ρ_b^N is the total baryon density in the NM phase. For given values of ρ_b^N and electron density ρ_e , the proton fraction x_p is determined from the β -equilibrium condition. In the case of quark matter phase, the equations of state are given by Eqs. (20) and (21). The total charge density ρ_z^Q in this phase is $\rho_z^Q = (2\rho_u - \rho_d - \rho_s)/3 - \rho_e$, where the flavour densities are as defined in Eq. (10). For given values of $\rho_b^Q (= \rho_q/3 = (\rho_u + \rho_d + \rho_s)/3)$ and ρ_e , the asymmetry parameters δ_{ud} and δ_{us} are determined from the β -equilibrium conditions given by Eq. (18).

The two conserved charges of this uniform droplet phase are the total baryon number and the total charge. The corresponding baryon density ρ_b and charge density ρ_z are expressed in terms of the volume fraction χ as:

$$\rho_z = \chi \rho_z^Q + (1 - \chi) \rho_z^N, \quad (34)$$

$$\rho_b = \chi \rho_b^Q + (1 - \chi) \rho_b^N. \quad (35)$$

Global charge neutrality requires that $\rho_z = 0$. Thus for given values of ρ_b , χ and ρ_b^N , the electron density ρ_e is fixed by charge neutrality condition given by Eq. (34) and ρ_b^Q is determined from Eq. (35). To arrive at the EOS of the droplet phase at a given density ρ_b , χ and ρ_b^N are to be determined from mechanical and chemical equilibria. The chemical equilibrium between the NM and QM phases requires that $\mu_n = 2\mu_d + \mu_u$ and $\mu_p = \mu_d + 2\mu_u$. From mechanical equilibrium, one has $P_{QM} = P_{NM}$, where the pressures in the two phases are as defined in Eqs. (24) and (20,21). The total energy density ϵ_T of the droplet phase is given by

$$\epsilon_T = \chi \epsilon_{QM} + (1 - \chi) \epsilon_{NM}, \quad (36)$$

where ϵ_{QM} and ϵ_{NM} are calculated with the constraints of mechanical, chemical and β -equilibrium conditions as well as with the condition of global charge neutrality.

For the study of the hybrid stars, the parameters in the effective mass model and the bag model are chosen so that $(M/A)_{P=0} > 930$ MeV. The parameters chosen in the effective mass model are $n = 2/3$, $C = 125$ MeV $f m^{-2}$ and $m_s^0 = 250$ MeV. In the bag model, we have taken $B^{1/4} = 175$ MeV and $m_s^0 = 250$ MeV.

B. Results and Discussions

The droplet phase obtained with global charge neutrality condition (as detailed in Sect. V.A.) is found to be energetically more favourable than the mixed phase determined by the Gibbs criteria, where each of the two phases is separately charge neutral. This is illustrated, in the effective mass and bag models, in Figs. 5 and 6 respectively. The dashed line corresponds to the mixed phase as obtained by the common tangent method. It is seen that the droplet phase extends well beyond the mixed phase (dashed line). This was also noted in earlier studies [15,16]. In

the limits of low density ($\chi \rightarrow 0$) and high density ($\chi \rightarrow 1$), the droplet phase smoothly joins with the NM and QM equations of state respectively as it should.

It may be parenthetically noted that the “down-turn” behaviour in the quark matter EOS in the low density region in Fig. 5 is due to the choice of the parameter n . In the limit $\rho_b \rightarrow 0$, the quark energy density ϵ_q [Eq. (9)] behaves as,

$$\begin{aligned}\epsilon_q &\sim \frac{\rho_q^{5/3}}{m_q} + m_q \rho_q, \\ &\sim \rho_b^{n+5/3} + C \rho_b^{1-n}.\end{aligned}\tag{37}$$

If $n = 1$, in the limit $\rho_b \rightarrow 0$, $\epsilon_q \rightarrow C$ in agreement with the usual bag model result. For $n = 2/3$, in the limit $\rho_b \rightarrow 0$, $\epsilon_q \rightarrow 0$, and this causes the “down-turn” in the quark matter EOS. We have chosen $n = 2/3$ as the Dirac-scalar potential [Eq. (1)] is generally taken to be of harmonic oscillator type, *i.e.* $l = 2$.

We now explore the possible consequences of the presence of a droplet phase on the structure of the hybrid star. To do this, we solve the TOV equation using the EOS shown in Figs. 5 and 6. The baryon number density and mass distributions inside the star, corresponding to the maximum mass configuration, determined using the effective mass and bag models are shown in Figs. 7 and 8 respectively. The hybrid star structure in the effective mass is characterised by the central density $\rho_c = 0.83 \text{ fm}^{-3}$, the radius $R = 11.8 \text{ km}$ and maximum mass $M_{\text{max}} = 1.48 M_\odot$. In the bag model we have $\rho_c = 0.88 \text{ fm}^{-3}$, $R = 11.6 \text{ km}$ and $M_{\text{max}} = 1.52 M_\odot$. One sees from Figs. 7 and 8 that the droplet phase extends in both the models from $\sim 1 \text{ km}$ to $\sim 8 \text{ km}$, and stars contain a core of about 1 km made of only QM and a crust region of about 4 km made up of only NM. We find that the droplet phase encompasses most of the volume of the star in agreement with an earlier study [15]. In a recent study [17] using the color-dielectric model, it was however noted that the substantial part of the core of the star contains only QM, and the droplet occupies roughly 40% of the total volume. It must be stressed that these finer details are in general model-dependent. Finally, the main conclusion of this section is that with the correct treatment of quark chemical potentials, we find that the hybrid star properties as obtained within the bag and effective mass models are quite similar. For this reason, for the study on the effect of spin polarisation on droplet phase, done in the following section, we use only the standard bag model.

VI. SPIN POLARISED NUCLEAR MATTER AND HYBRID STARS

In this section, we explore the properties of the hybrid stars using the proposed NM equation of state given by Eqs. (26) and (27), which predicts a ferromagnetic phase transition at high densities.

A. Spin polarisation and droplet phase

Firstly, to know whether there exists a phase transition between the nuclear matter phase described by Eqs. (26,27) and the QM phase characterised by the bag model EOS, Eq. (21), we compare the total energies per baryon obtained in the two phases. The parameters chosen for this purpose are as given in section III.B for NM phase, and for QM, we have taken $B^{1/4} = 180 \text{ MeV}$ and $m_s = 250 \text{ MeV}$. Further, in the case of NM, the total energy is minimised with respect to both the neutron and proton spin polarisation parameters, α_n and α_p respectively. This energy minimised nuclear matter calculation is hereafter referred to as EMNM. In addition, we also calculated the total energies for unpolarised nuclear matter (UNM), where $\alpha_n = 0$ and $\alpha_p = 0$ at all densities. Results of these calculations are displayed in Fig. 9.

One can observe a slight bend in the EMNM curve at $\rho \sim 0.7 \text{ fm}^{-3}$. This point indicates the ferromagnetic phase transition density, ρ_{FM} , where the optimum value of α_n sharply increases from zero to unity. (This feature is clearly illustrated in Fig. 3 of Ref. [18].) It is also seen that a polarised nuclear matter (PNM) phase is energetically favourable over the density region $\rho_{\text{FM}} \leq \rho \leq \rho_{\text{HQ}}$, where $\rho_{\text{HQ}} \simeq 10\rho_0$ is the NM-QM phase transition density. It would be interesting to know whether there exists a droplet phase consisting of droplets of SQM and PNM. For this purpose, we made an attempt to solve for the droplet phase following the same procedure detailed in section V. It was then found that there exists no solution for phase equilibrium between SQM and PNM phases. In order to understand this result, we do the following analysis.

Firstly, to show the effect of increasing proton fraction on α_n , we calculated, for given values of x_p and ρ_b , the optimum value of α_n by energy minimisation. Values of α_n so determined are plotted in Fig. 10 as a function of density for few values of x_p . (It may be said here that for $x_p \leq 0.5$, values usually found in the droplet phase, the

maximum of the optimum value of α_p , obtained with increase in density, is very nearly zero.) As x_p increases, the value of ρ_{FM} increases and the maximum value of α_n , given by $(1 - x_p)$, decreases. Therefore, in general, one might say that NM phase with large value of x_p disfavours spin polarisation. On the otherhand, as it was noted [18] before, as NM gets spin polarised the β -equilibrated x_p sharply falls to zero, which is also evident from Fig. 11, where we have shown mass per baryon versus density for certain cases. One can see that there is a slight deviation, for densities $\rho_b < \rho_{\text{FM}}$, between the EMNM (with $x_p = 0$) curve and the EMNM curve obtained taking β -equilibration into account, which is essentially due to non-zero, though small, values of x_p . However, as density is increased further, the two curves coincide exactly illustrating the fact that β -equilibrated x_p values become zero at $\rho \simeq \rho_{\text{FM}}$. Another interesting aspect is that beyond the ferromagnetic transition density, the PNM phase is energetically more favourable than the UNM with large values of x_p . Hence, for densities $\rho_b > \rho_{\text{FM}}$, droplets of UNM with $x_p > 0$ would prefer to become PNM with $x_p = 0$. That is, one expects a transition from a state ($x_p > 0, \alpha_n = 0$) to a state ($x_p = 0, \alpha_n \simeq 1$). But, this change of state, in the context of formation of a DP, is disallowed for the following reasons.

In contrast to the usual mixed phase defined by the common tangent method, in the case of a droplet phase, the electron density is same both in NM and QM phases. Restricting to densities $\rho_b > \rho_{\text{FM}}$, the following three cases are considered.

CASE 1 : Firstly, let us consider the simplest situation with $\mu_e = 0$ and $N_e = 0$, where we have neglected the small e^- mass. Then, the optimum configuration for QM phase gives $\mu_u = \mu_d = \mu_s$ and $N_u = N_d = N_s$, where we have taken $m_u = m_d = m_s$. For the NM phase, at $\rho_b > \rho_{\text{FM}}$, the optimum configuration gives $x_p = 0$ and $\alpha_n = 1$. Thus, one finds that the two phases are separately charge neutral, and hence corresponds to the usual mixed phase with $N_e = 0$.

CASE 2 : Secondly, let us consider as in case 1, $\mu_e = 0$ and $N_e = 0$. But now, we insist that $m_s > m_d = m_u$. Then the optimum configuration for the QM phase gives $\mu_u = \mu_d = \mu_s$ with $N_s < N_d = N_u$, and thereby the QM droplets are now positively charged. For the global charge neutrality condition to be satisfied, the NM droplets should be negatively charged. However, according to the optimum configuration, the NM droplets consists of only spin polarised neutrons. Therefore, in this case, there exists no DP solution.

CASE 3 : Finally, let us consider the general situation, where $\mu_e \neq 0$ (and $N_e \neq 0$), and $m_s > m_d = m_u$. Now with finite electron density, the β -equilibrium condition pertaining to the NM droplets, at a density ρ_b , is given by $(1/\rho_b) d\epsilon_n/dx_p + \mu_e = 0$. Since $\mu_e > 0$, the slope factor $d\epsilon_n/dx_p$ must be negative. From Fig. 12, it can be seen that this is satisfied for the configuration UNM, i.e. $x_p \sim 0.5$ and $\alpha_n = 0$. This then suggests that NM droplets with $\rho_b > \rho_{\text{FM}}$ in DP may remain unpolarised with $x_p > 0$, which however is not the optimum configuration for NM phase. Thus, due to the nature of droplet phase, that is, constancy of electron density in both phases, and the interplay of x_p and α_n , one finds that NM droplets with $\rho_b > \rho_{\text{FM}}$ in DP may remain unpolarised with $x_p > 0$. It may be remembered that the usual mixed phase between SQM and PNM however exists. In the following subsection, we explore the possibility of forming a DP with UNM phase and SQM phase.

B. Properties of hybrid stars

From our earlier study on hybrid stars, it can be seen (from Table 2 of Ref. [18]) that for the chosen set of parameters, the central density of the star is about $6\rho_0$. Therefore, the UNM-SQM phase transition at $\rho \simeq 0.8 \text{ fm}^{-3}$ is of more relevance. Following the same procedure described in section V, we then solved the set of simultaneous equations corresponding to β -equilibrium, charge neutrality, chemical and mechanical equilibria. Results obtained for the droplet phase along with the usual mixed phase are shown in Fig. 13. It can be seen that as in other cases, the droplet phase extends well beyond the mixed phase. Interestingly, the droplet phase is energetically favourable even than the EMNM case over the region $0.5 \leq \rho \leq 0.9$. Further, in this particular case, only a part of DP is allowed as EMNM configuration takes over at high densities. Thus, one has according to the minimum energy criterion, a DP sandwiched between UNM and PNM phases. We now explore the possible consequences of the presence of a DP on the structure of hybrid stars.

In Fig. 14, we show the proton fraction obtained in the DP using the realistic interaction [Eq. (25)], and compare with the one obtained within the simple parametrisation [Eq. (24)]. It can be seen that the general trend is quite similar in both the cases. Values of x_p as obtained with the realistic interaction is somewhat lower than the simple one. As the bag model parameters are more or less the same, this could be due to the fact that the EOS based on realistic interaction is relatively softer than the simple parametrised EOS. Nevertheless, values of x_p is high enough to allow for direct URCA process to happen. We now solve the TOV equation (32) using the EOS shown in Fig. 13, and obtain the structural properties such as mass and size of the star. The baryon number density and mass distribution inside the star, corresponding to the maximum mass configuration, are plotted in Fig. 15. The maximum mass configuration is characterised by the central density $\rho_c = 1.02 \text{ fm}^{-3}$, the radius $R = 11.4 \text{ km}$ and maximum

mass $M_{\text{max}} = 1.62M_{\odot}$. Now, from Fig. 15, one observes that there exists a mixed phase consisting of droplets of SQM and UNM sandwiched between a PNM core and UNM crust. The droplet phase extends from $\sim 2 \text{ km}$ to $\sim 6 \text{ km}$. More interestingly, there exists also a core of about 1 km consisting PNM. Thus, the salient features of this star structure are the following. Firstly, the mass and size of the star obtained in the present calculation is well within the acceptable limits. Secondly, due to the presence of a droplet phase, the value of x_p found inside the star allows direct URCA process to happen, and thereby have important consequences on the cooling process of neutron stars. Finally, due to the presence of a spin polarised core, we could also, in principle, explain the surface magnetic field of neutron stars. Value of the magnetic field at the surface of the star due to the presence of a ferromagnetic core can be estimated using the relation $H \sim \alpha_n \mu_n N / R^3$, where $N \simeq 1.4 \times 10^{54}$ is the number of neutrons in the ferromagnetic phase and $R \simeq 11.4 \text{ km}$ is the star size. Then using $|\mu_n| = 1.91$ nuclear magneton, we get $H \sim 10^{13} \text{ G}$. Thus, the surface magnetic field is somewhat overestimated compared to the observed value $\sim 10^{12} \text{ G}$. However, by fine-tuning the parameter E_Y , as ρ_{FM} is sensitive to this parameter, one could arrive at the right value.

Before summarising our findings, we would like to stress that the star's internal structure very much depends upon the model parameters chosen. For example, keeping E_Y fixed at 15 MeV, and decreasing the bag parameter from 180 MeV to 170 MeV, one can see from Fig. 16 that PNM phase is no more allowed by energy minimum criterion. On the otherhand, with the bag parameter fixed at 180 MeV and increasing E_Y from 15 MeV to 17 MeV, one finds that, though there exists a small density region where DP is favoured, PNM phase occupies larger phase space than the DP as illustrated in Fig. 17. Hence, in this case, the surface magnetic field will be largely overestimated. However, within an allowed set of parameters, we could, in principle, quite satisfactorily explain the structural properties, surface magnetic field as well as allow for the formation of a DP.

VII. SUMMARY

To summarize, firstly, we have constructed a quark matter equation of state in the effective mass approximation and then applied it to investigate some properties of strange quark matter with particular reference to hybrid and strange quark stars. In this effective mass model, the quark masses are chosen to be density dependent and the absolute confinement of quarks as well as the asymptotic freedom are adequately taken care of through this density dependence. With these effective masses, it is seen that the chemical potential acquires an extra term, the so-called rearrangement term. Presence of such a term in the single particle energy is consistent with the well-known Hugenholtz-Van Hove theorem. Thus, the present calculation, in contrast to earlier studies, correctly treats the quark chemical potentials in the effective mass model.

Secondly, we make a comparative study of hybrid star properties as obtained within the effective mass and bag models. For nuclear matter equation of state, we first used a simple parametrisation. It is found that a well-defined mixed phase of droplets of quark and nuclear matter sandwiched between a pure quark matter core and a crust of only nuclear matter exists. This mixed phase is found to occupy most of the volume of the star. The main result of this comparative study is that both the bag and effective mass models yield similar results.

Thirdly, using a realistic equation of state of nuclear matter based on a finite range, momentum and density dependent (FRMDD) interaction, which predicts a ferromagnetic phase transition at a density $\rho_b \sim 4\rho_0$, we investigated the effect of spin polarisation on the formation of a droplet phase. It is found that as nuclear matter gets polarised, the value of proton fraction x_p drops sharply to zero, or vice versa, as x_p increases, the transition density ρ_{FM} increases and hence matter with $x_p > 0$ prefers to remain unpolarised. Because of this interplay between α_n and x_p , there exists no mixed phase consisting of droplets of strange quark matter and polarised nuclear matter.

Finally, using the same equation of state based on FRMDD interaction alongwith the usual bag model, we find that a droplet phase consisting of strange quark matter and unpolarised nuclear matter can however exist. This droplet phase is sandwiched between a core made up of polarised nuclear matter and a crust containing unpolarised nuclear matter. This, in principle, allows for a satisfactory explanation of the structural properties and surface magnetic field of neutron stars and keeps room for their rapid cooling due to the direct URCA process.

Acknowledgements : The authors are grateful to Amand Faessler for his valuable comments and suggestions. One of us (V.S.U.), gratefully acknowledges the Institute of Theoretical Physics of University of Tuebingen for financial support, where a part of this work was completed.

-
- [1] A. Hewish, S.J. Bell, J.D.H. Pilkington, P.F. Scott, and R.A. Collins, *Nature* **217** (1968) 709.
- [2] T. Gold, *Nature* **218** (1968) 731; **221** (1969) 25.
- [3] M. Prakash, *Nuclear equation of state*, Eds. A. Ansari and L. Satpathy, (World Scientific, Singapore, 1996).
- [4] S.L. Shapiro and S.A. Teukolsky, *Black holes, white dwarfs and neutron stars* (Wiley, New York, 1983).
- [5] N. Itoh, *Prog. Theor. Phys.* **44** (1970) 291.
- [6] K. Brecher and G. Caporaso, *Nature* **259** (1976) 378.
- [7] G. Baym and S. Chin, *Phys.Lett.***62B** (1976) 241.
- [8] B. Freedman and L. McLerran, *Phys.Rev.***D17** (1978) 1109.
- [9] C. Alcock, E. Farhi, and A. Olinto, *Astrophys.J.* **310** (1986) 261.
- [10] P. Haensel, J.L. Zdunik, and R. Schaeffer, *Astron. Astrophys.* **160** (1986) 121.
- [11] N.K. Glendenning, *Phys.Rev.Lett.***63** (1987) 1825.
- [12] E. Witten, *Phys.Rev.***D30** (1984) 272.
- [13] X. D. Li, Z. G. Dai, and Z. R. Wang, *Astron. Astrophys.* **303** (1995) L1-L4.
- [14] J. Madsen, *astro-ph* 9601129.
- [15] N.K. Glendenning, *Phys.Rev.***D46** (1992) 1274; *Phys.Rep.* **264** (1996) 143.
- [16] H. Heiselberg, C.J. Pethick, and E.F. Staubo, *Phys. Rev. Lett.* **70** (1993) 1355.
- [17] A. Drago, U. Tambini, and M. Hjorth-Jensen, *Phys.Lett.* **B380** (1996) 13.
- [18] V.S. Uma Maheswari, D.N. Basu, J.N. De, and S.K. Samaddar, *Nucl. Phys.* **A 615** (1997) 516.
- [19] A. Chodos, R.L. Jaffe, K. Johnson, C.B. Thorn and V.F. Weisskopf, *Phys.Rev.***D9** (1974) 3471.
- [20] K.A. Olive, *Nucl.Phys.***B190** (1981) 483.
- [21] G.N. Fowler, S. Raha, and R.M. Weiner, *Z.Phys.***C9** (1981) 271.
- [22] D.H. Boal, J. Schachter and R.M. Woloshyn, *Phys.Rev.* **D26** (1982) 3245.
- [23] S. Chakrabarty, *Phys.Rev.***D43** (1991) 627; *Nuovo Cimento* **106B** (1991) 1023.
- [24] O.G. Benvenuto and G. Lugones, *Phys.Rev.***D51** (1995) 1989.
- [25] M.B. Christiansen and N.K. Glendenning, *astro-ph/9706056*.
- [26] V.S. Uma Maheswari, *Phys. Rev.* **D 54** (1996) 3389.
- [27] G. tHooft, *Nucl.Phys.***B72** (1974) 461; *Phys.Rev.***D14** (1976) 3432.
- [28] R. Tegen, *Ann.Phys.***197** (1990) 439.
- [29] Y. Nambu and G. Iona-Lasinio, *Phys.Rev.***122** (1961) 345; **124** (1961) 246.
- [30] B.C. Parija, *Phys.Rev.***C45** (1992) 415.
- [31] A. Bohr and B. Mottelson, *Nuclear Structure*, (Benjamin Inc., Amsterdam), (1969).
- [32] D. Bandyopadhyay, C. Samanta, S.K. Samaddar and J.N. De, *Nucl. Phys.***A511**(1990) 1.
- [33] N.M. Hugenholtz and L. Van Hove, *Physica(Utrecht)* **24** (1958) 363.
- [34] P. Haensel, *Z.Phys.***A274** (1975) 377.
- [35] M. Abd-Alla, S. Ramadan and M.Y. Hassan, *Phys.Rev.***C36**(1987) 1565.
- [36] H. Uberall, *Electron scattering from complex nuclei*, (N.Y.), Academic Press (1971).
- [37] M.M. Majumdar, S.K. Samaddar, N. Rudra and J.N. De, *Phys.Rev.***C49** (1994) 541.
- [38] B. Friedman and V.R. Pandharipande, *Nucl.Phys.***A361** (1981) 502.
- [39] R.B. Wiringa, V. Fiks and A. Fabrocini, *Phys.Rev.***C38** (1988) 1010.
- [40] R.P. Feynman, N. Metropolis and E. Teller, *Phys.Rev.***75**(1949) 1561.
- [41] G. Baym, C. Pethick and P. Sutherland, *Astrophys.J.***170**(1971) 299.
- [42] G. Baym, H.A. Bethe and C.J. Pethick, *Nucl.Phys.***A175** (1971) 225.

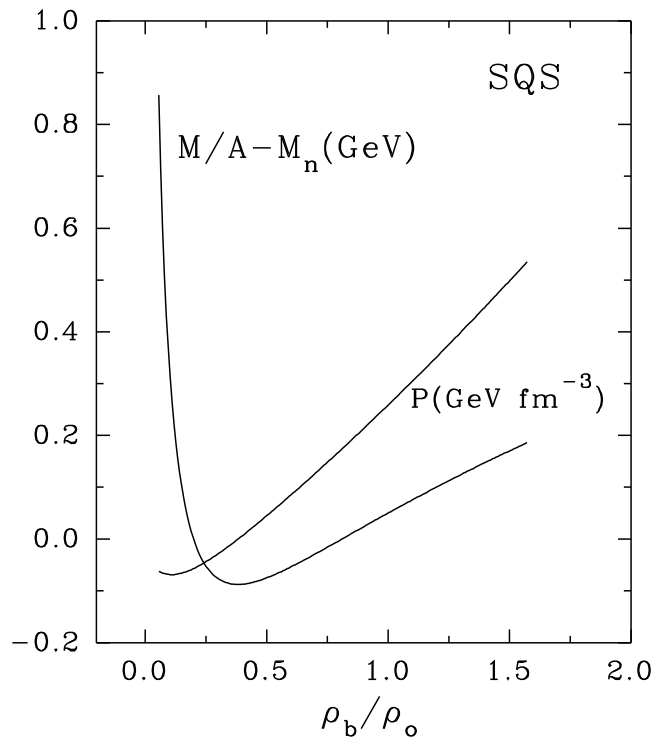


FIG. 1. Total mass per baryon M/A and total pressure P corresponding to flavour symmetric strange quark matter is shown as a function of baryon density ρ_b in the effective mass model. M_n is the nucleon mass and ρ_o is the normal nuclear matter density.

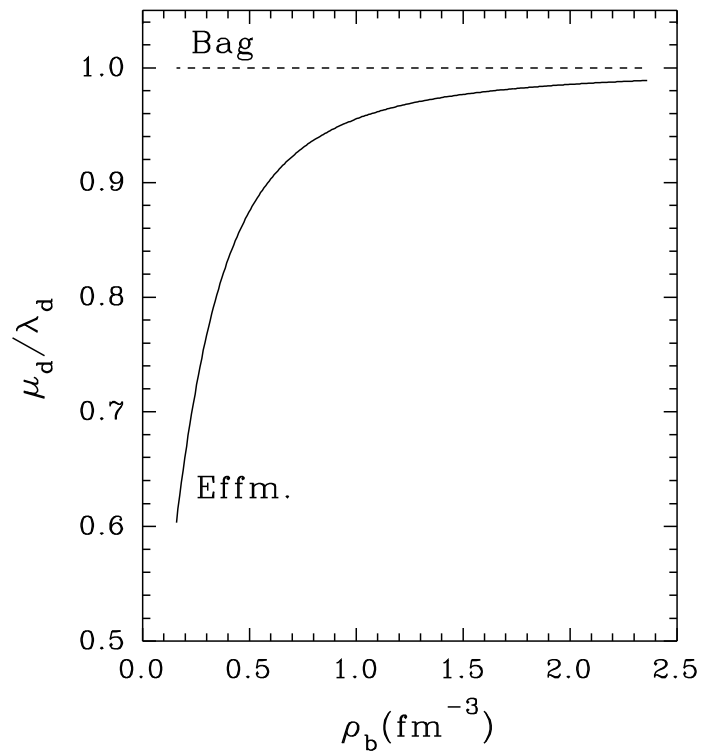


FIG. 2. Quark chemical potential [see Eq. (17)] obtained in the effective mass and bag models are shown as a function of baryon density ρ_b .

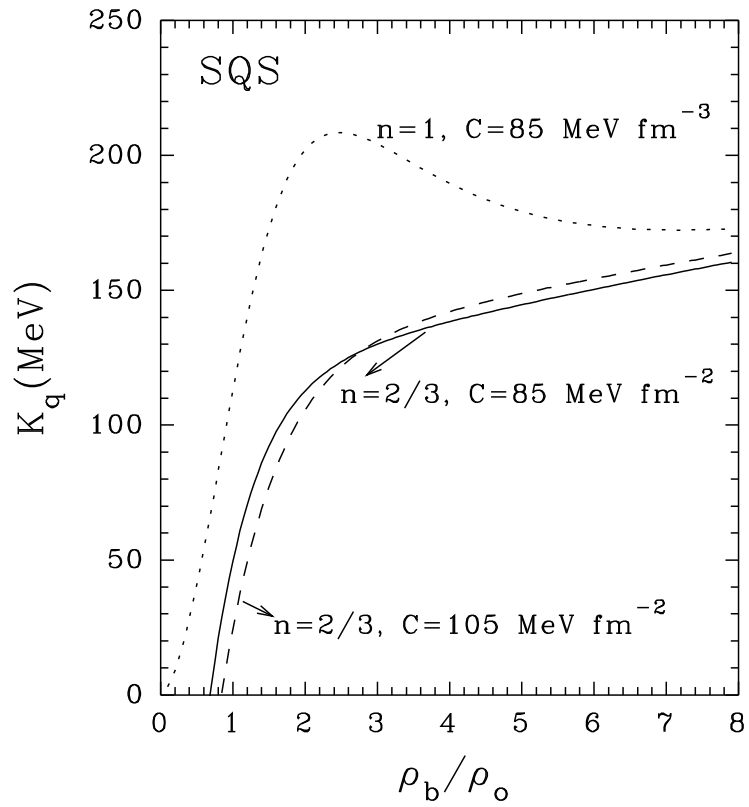


FIG. 3. Incompressibility K_q of flavour symmetric strange quark matter is shown as a function of baryon density ρ_b in the effective mass model. Values of the mass parameters n and C chosen are given. ρ_o is the normal nuclear matter density.

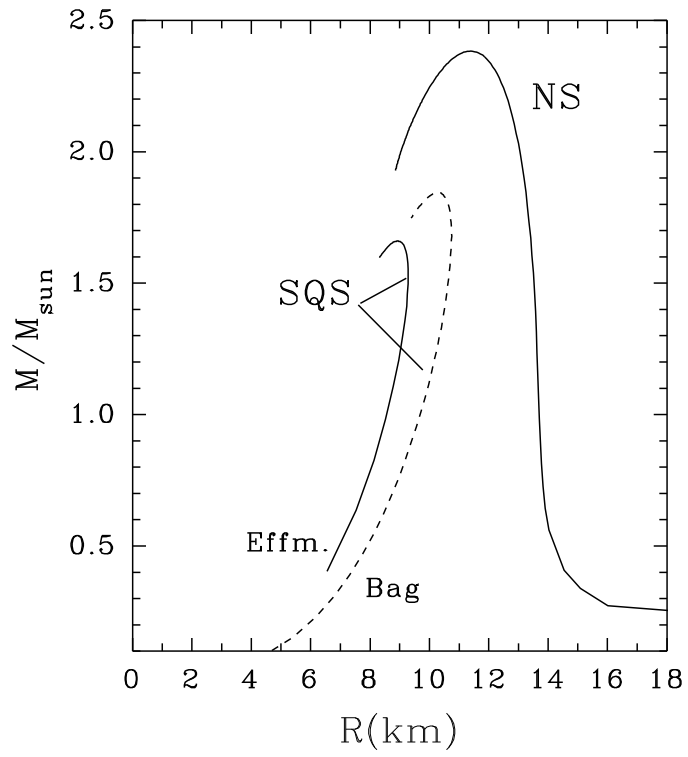


FIG. 4. Mass-radius relationships of strange quark stars (SQS) as obtained in effective mass and bag models are compared with a neutron star (NS) one.

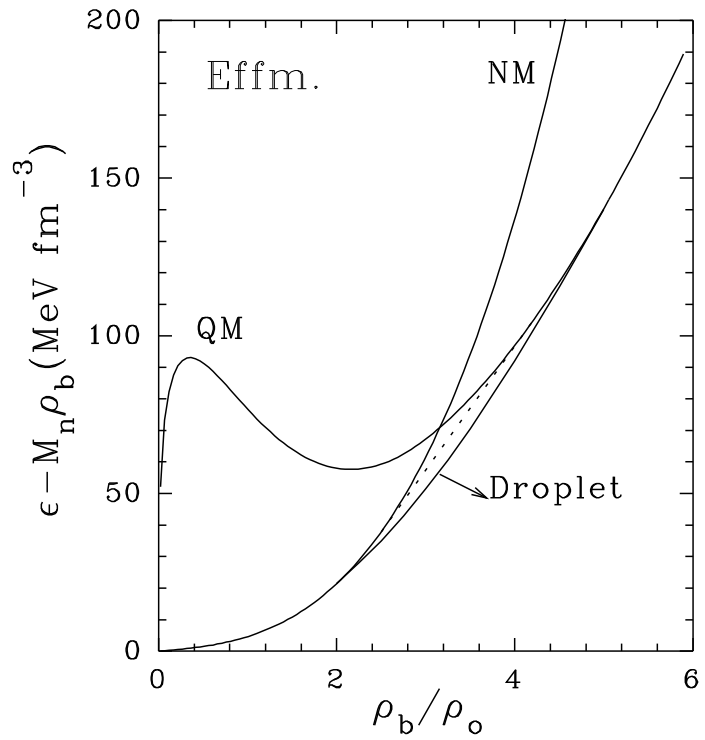


FIG. 5. Total energy densities of nuclear matter (NM), quark matter (QM) and droplet phase are shown as a function of baryon density ρ_b in the effective mass model. The dashed line represents the mixed phase obtained by common tangent method. M_n is the nucleon mass.

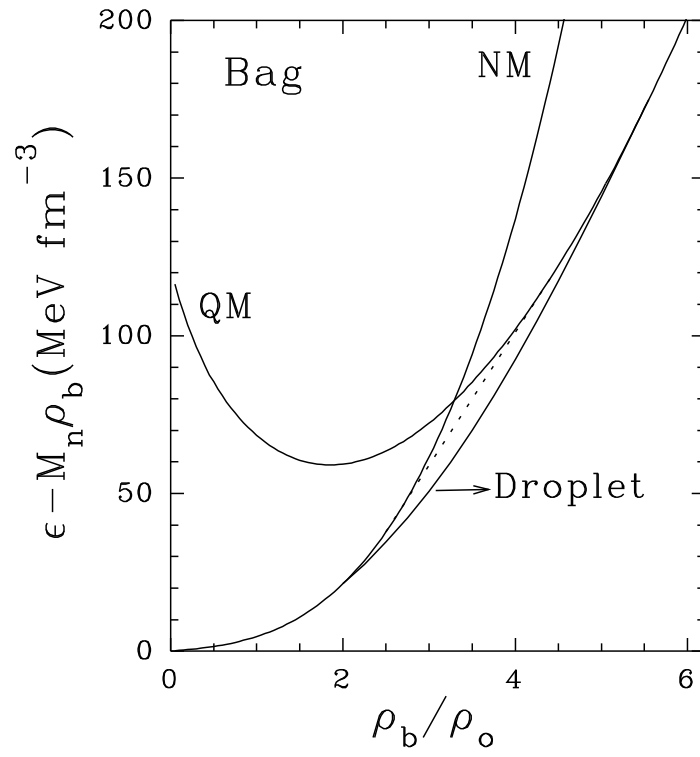


FIG. 6. Same as in Fig. 5, but for the bag model.

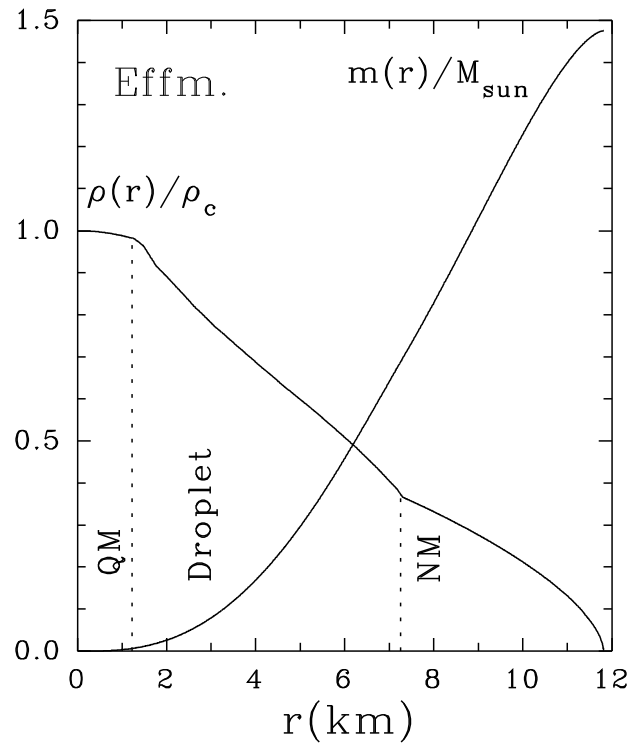


FIG. 7. Baryon density [$\rho(r)$] and mass [$m(r)$] distributions corresponding to the maximum mass configuration are shown as a function of the radial distance r in the effective mass model. $M_{\text{sun}}(\equiv M_{\odot})$ is the solar mass and ρ_c is the baryon density at the core ($r = 0$) of the star.

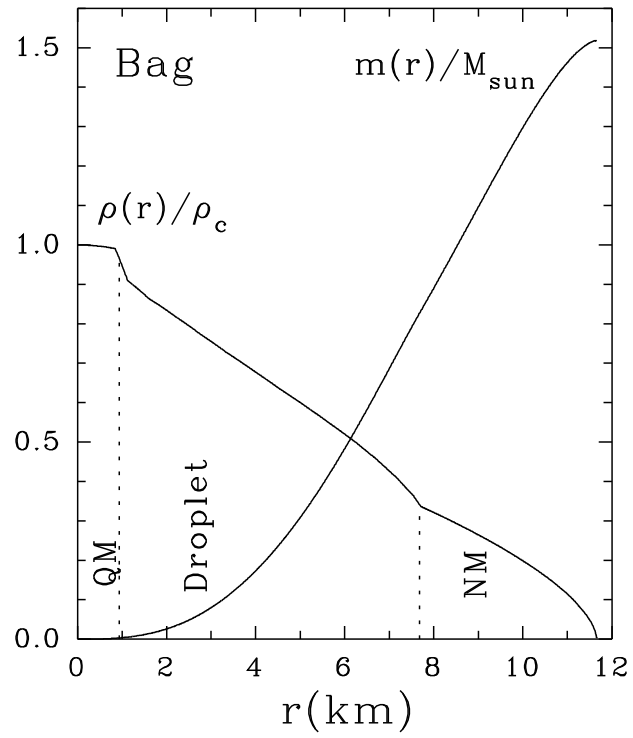


FIG. 8. Same as in Fig. 7, but for the bag model.

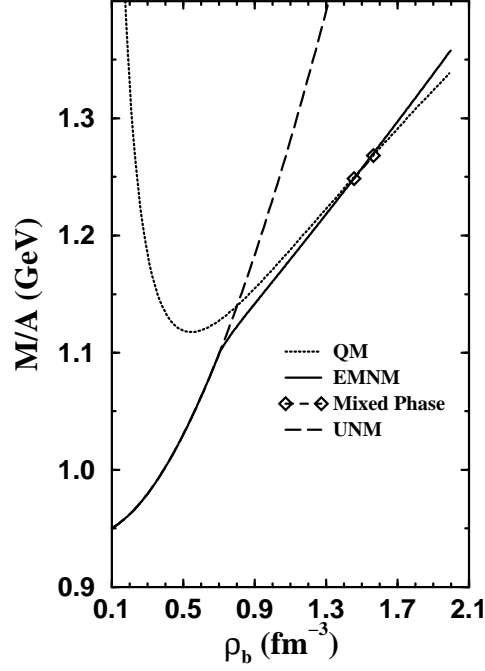


FIG. 9. Total mass energies per baryon of quark matter (QM), nuclear matter minimised with respect to spin polarisation parameters (EMNM), unpolarised nuclear matter (UNM) and mixed phase are shown as a function of baryon density ρ_b . Parameters chosen are : $B^{1/4} = 180 \text{ MeV}$, $m_s = 250 \text{ MeV}$ and $E_Y = 15 \text{ MeV}$.

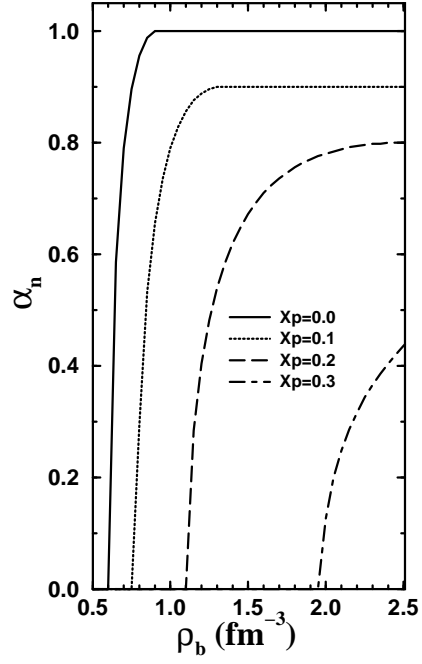


FIG. 10. The value of spin polarisation parameter α_n obtained from minimisation of energy for particular values of x_p .

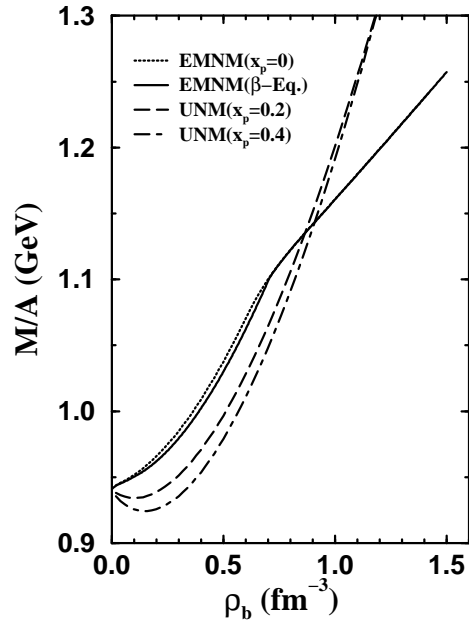


FIG. 11. Mass energies per baryon obtained for pure neutron matter ($x_p = 0$) and β -equilibrated nuclear matter (solid line) considering energy minimisation with respect to spin polarisation parameters are shown. Results obtained for unpolarised nuclear matter (UNM) with particular values of proton fraction x_p are also plotted.

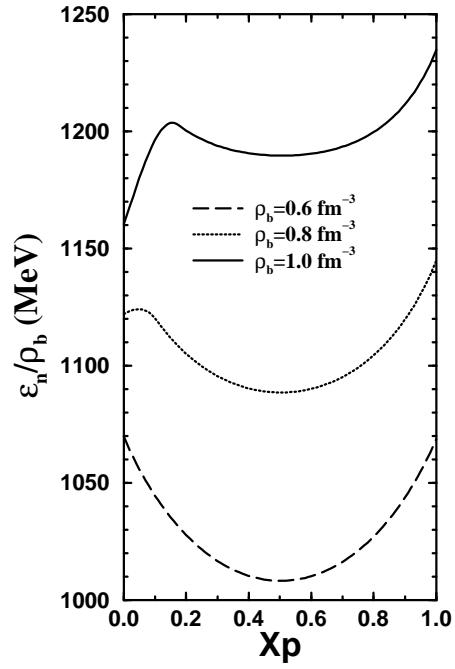


FIG. 12. Total energy density ϵ_n of nuclear matter obtained considering energy minimisation with respect to spin polarisation parameters are shown as a function of proton fraction x_p for three particular values of baryon density ρ_b .

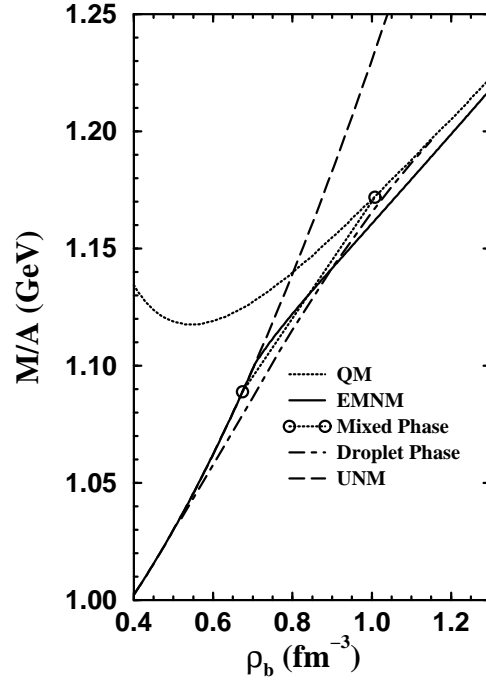


FIG. 13. Same as in Fig. 9, but the droplet phase consisting of unpolarised nuclear matter and strange quark matter droplets are also shown.

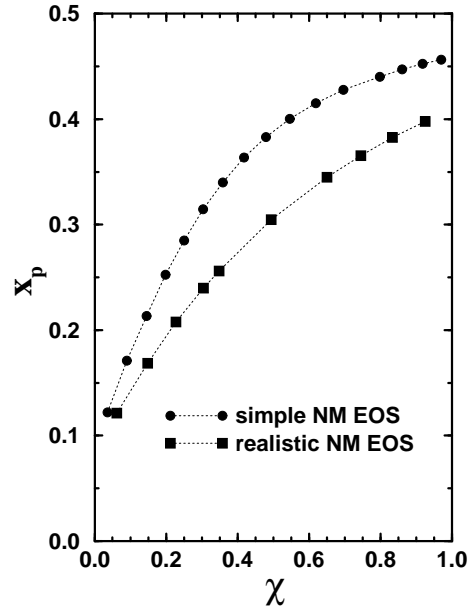


FIG. 14. Values of proton fraction x_p obtained for droplet phase using bag model equation of state (EOS) for quark matter, and with a simple parametrised EOS (24) and a realistic one (26,27) for nuclear matter are shown as a function of volume fraction χ .

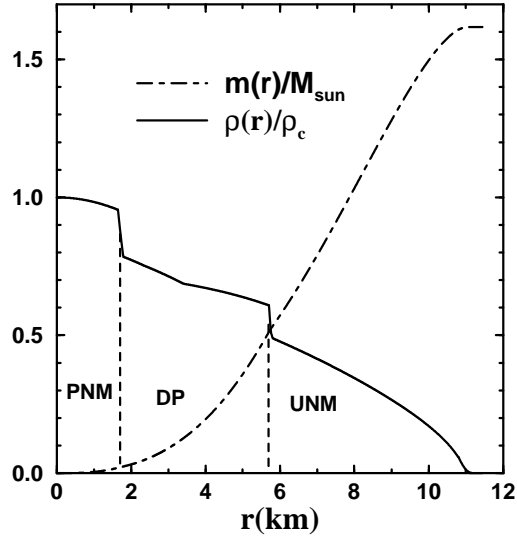


FIG. 15. Baryon density $[\rho(r)]$ and mass $[m(r)]$ distributions corresponding to the maximum mass configuration obtained with bag model (21) and realistic nuclear matter (26,27) equations of state are shown as a function of the radial distance r . $M_{\text{sun}}(\equiv M_{\odot})$ is the solar mass and ρ_c is the baryon density at the core ($r = 0$) of the star. (For details see section VI.)

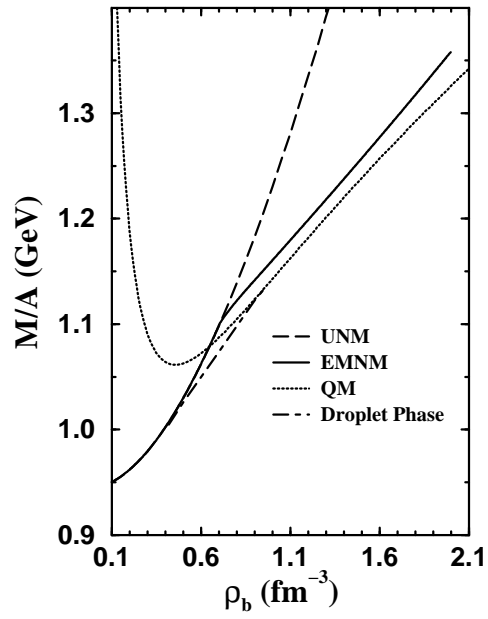


FIG. 16. Same as in Fig. 9, but with $B^{1/4} = 170 \text{ MeV}$.

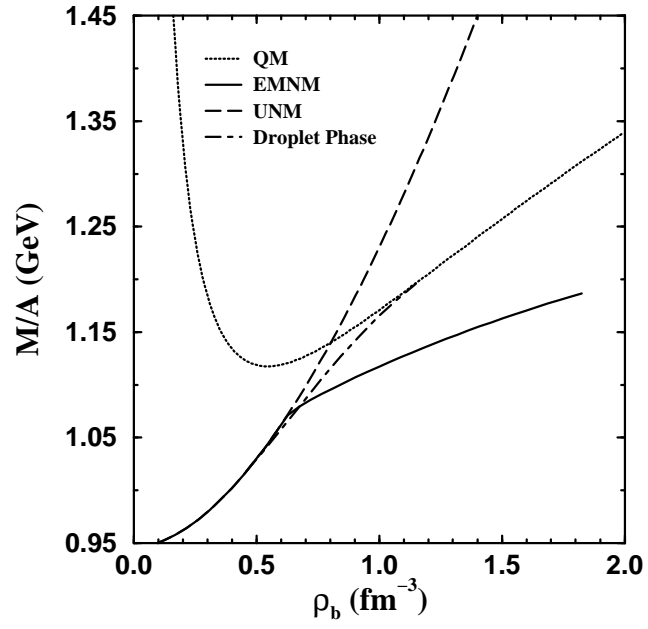


FIG. 17. Same as in Fig. 9, but with $E_Y = 17 \text{ MeV}$.

n	C ($MeV fm^{-3n}$)	$(M/A)_{P=0}$ (MeV)	ρ_c/ρ_o	R (km)	M_{max}/M_\odot
$\frac{1}{3}$	127	860.0	7.31	10.5	1.85
	137	893.3	8.20	9.7	1.71
	147	925.3	9.10	9.1	1.60
$\frac{2}{3}$	85	851.6	8.25	9.8	1.86
	95	883.8	9.22	9.1	1.73
	105	913.8	10.18	8.5	1.62
1	65	855.6	8.72	9.4	1.86
	75	886.8	9.71	8.8	1.73
	85	914.9	10.66	8.2	1.62

TABLE I. Values of mass per baryon of flavour symmetric strange quark matter at zero pressure $(M/A)_{P=0}$, and central density ρ_c , radius R and mass M_{max} corresponding to the maximum mass configuration of the strange quark star are given for few sets of the mass parameters (n, C) . ρ_o is the normal nuclear matter density.